MOLECULAR AND CELLULAR BIOLOGY, Sept. 2011, p. 3639–3652 Vol. 31, No. 17
0270-7306/11/$12.00 doi:10.1128/MCB.05429-11

Regulation of Androgen Receptor-Mediated Transcription by RPB5 Binding Protein URI/RMP▽

Paolo Mita,[1] Jeffrey N. Savas,[2] Nabil Djouder,[5] John R. Yates III,[2] Susan Ha,[1,3] Rachel Ruoff,[1,3] Eric D. Schafler,[1] Jerome C. Nwachukwu,[4] Naoko Tanese,[6] Nicholas J. Cowan,[7] Jiri Zavadil,[8] Michael J. Garabedian,[3,6] and Susan K. Logan[1,3]*

Departments of Pharmacology,[1] Urology,[3] Microbiology,[6] and Biochemistry,[7] New York University School of Medicine, and Department of Pathology and NYU Center for Health Informatics and Bioinformatics, New York University Langone Medical Center,[8] New York, New York 10016; Department of Chemical Physiology, The Scripps Research Institute, La Jolla, California[2]; The Scripps Research Institute, Jupiter, Florida[4]; and 5 Centro Nacional de Investigaciones Oncológicas, CNIO, Fundación Banco Bilbao Vizcaya (F-BBVA)-CNIO Cancer Cell Biology Programme, E-28029 Madrid, Spain[5]

Received 30 March 2011/Returned for modification 2 May 2011/Accepted 21 June 2011

Androgen receptor (AR)-mediated transcription is modulated by interaction with coregulatory proteins. We demonstrate that the unconventional prefoldin RPB5 interactor (URI) is a new regulator of AR transcription and is critical for antagonist (bicalutamide) action. URI is phosphorylated upon androgen treatment, suggesting communication between the URI and AR signaling pathways. Whereas depletion of URI enhances AR-mediated gene transcription, overexpression of URI suppresses AR transcriptional activation and anchorage-independent prostate cancer cell growth. Repression of AR-mediated transcription is achieved, in part, by URI binding and regulation of androgen receptor trapped clone 27 (Art-27), a previously characterized AR corepressor. Consistent with this idea, genome-wide expression profiling in prostate cancer cells upon depletion of URI or Art-27 reveals substantially overlapping patterns of gene expression. Further, depletion of URI increases the expression of the AR target gene NKX-3.1, decreases the recruitment of Art-27, and increases AR occupancy at the NKX-3.1 promoter. While Art-27 can bind AR directly, URI is bound to chromatin prior to hormone-dependent recruitment of AR, suggesting a role for URI in modulating AR recruitment to target genes.

Widespread interest in the mechanism of transcriptional regulation by the androgen receptor (AR) has been stimulated by the finding that AR signaling is critically important in the progression of both androgen-dependent and castration-resistant prostate cancers (2, 9). Cofactors, corepressors, and/or coactivators are responsible for the regulation of AR-mediated transcription, and therefore, their misregulation or aberrant expression can impact tumor formation and progression.

Recent studies identified the TMPRSS2-ETS fusion as a specific chromosomal alteration highly represented in prostate cancer (27). Fusion of the androgen-responsive TMPRSS2 gene promoter with the coding region of ETS transcription factors leads to aberrant androgen regulation of ETS target genes. One of these target genes was reported to be C19orf2, coding for the unconventional prefoldin RPB5 interactor (URI) (26).

URI was originally identified as a protein that binds the RPB5 subunit of RNA polymerases (8). It also binds other nuclear proteins involved in transcription, including the general transcription factor IIF (TFIIF) (15, 30) and components of the Paf-1 complex that promote polymerase II (pol II) phosphorylation and histone modifications during elongation (33). Although URI was initially demonstrated to function as a transcriptional repressor (8), its role in transcriptional regulation is not well understood. One clue may be that the yeast homologue of URI, Bud27, plays an essential role in the assembly of a multiprotein complex that includes the jumanji demethylase Gis1 (28). In addition, overexpressed URI interacts with DNA methyltransferase-associated protein 1 (DMAP1), a protein shown to be involved in the nuclear translocation of URI (5). In fact, URI is a multifaceted protein, and reports have linked URI to numerous cellular processes, including nutrient response downstream of the mammalian target of rapamycin (mToR) pathway (11), translation initiation (6), apoptosis through the binding and regulation of protein phosphatase 1 (PP1) (7, 14), and the DNA damage response (20). These findings indicate that URI and its associated proteins represent an important node among cellular pathways that integrates nutrient sensing, cellular stress, and cell death (12). In addition, a recent report identified a cytoplasmic Hsp90 and R2TP/prefoldin-like complex containing URI that was proposed to be involved in the cytoplasmic assembly of RNA polymerase II (1).

Although multiple laboratories have shown by immunoprecipitation and mass spectrometry that URI interacts with RNA polymerase (3, 13) and is recruited to sites of active transcription in polytene chromosomes in *Drosophila* (14), very little is known about the role URI plays in regulating transcription. In this report, we investigate the impact of URI on AR agonist-

* Corresponding author. Mailing address: Departments of Urology and Pharmacology, New York University School of Medicine, 550 First Avenue, MSB424, New York, NY 10016. Phone: (212) 263-2921. Fax: (212) 263-7133. E-mail: susan.logan@nyumc.org.
▽ Published ahead of print on 5 July 2011.

and antagonist-mediated gene transcription in prostate cancer cells. We find that URI represses AR-mediated transcription and that loss of URI diminishes antiandrogen transcriptional repression. Overexpression of URI also inhibits anchorage-independent growth of androgen-dependent prostate cells, supporting a role for URI as an AR repressor. We demonstrate that URI interacts with the AR corepressor Art-27 and that disruption of either protein destabilizes the other. Microarray analysis upon URI or Art-27 loss shows overlapping effects on AR-mediated gene transcription. These data suggest that the effect of URI on AR-dependent transcription is, in part, mediated by Art-27. Moreover, we observe that the URI/Art-27 complex can bind chromatin independently of AR and that loss of URI results in increased recruitment of AR, suggesting that transcriptional regulation via URI and Art-27 might occur through multiple mechanisms.

MATERIALS AND METHODS

Cell culture and stable cell lines. LNCaP cells were cultured in a complete medium: RPMI 1640 (Cellgro) supplemented with 10% fetal bovine serum (FBS; HyClone) and 1% penicillin-streptomycin (Cellgro). HEK293 and PC3 cells were cultured in Dulbecco's modified Eagle's medium (DMEM; Cellgro), and F-12 (Ham) medium (Invitrogen), respectively, supplemented with 10% FBS and 1% penicillin-streptomycin. Rapamycin was purchased from Sigma-Aldrich and AKT inhibitor VIII from EMD Biosciences.

LNCaP cells or HEK293 cells stably overexpressing the FLAG-URI alpha construct (7) or an empty vector were generated by transfecting cells with pcDNA3-FLAG-URI or the empty vector pcDNA3 using Lipofectamine 2000 (Invitrogen). Forty-eight hours posttransfection, cells stably overexpressing the construct were selected with Geneticin (500 μg/ml; Invitrogen) for 15 days.

LNCaP cells in which reduced expression of URI is inducible by doxycycline were generated with lentiviral pTRIPZ short hairpin RNA (shRNA) against URI (RHS4696-99683127; Open Biosystems) or a control shRNA (RHS4743; Open Biosystems). After infection, cells were selected for 10 days with 1 μg/ml puromycin (Sigma-Aldrich). In addition, stable cell line pools were screened for inducible knockdown of URI using 1 μg/ml doxycycline (Sigma-Aldrich).

Immunohistochemistry, immunoblotting, and immunoprecipitation. Human prostate samples were obtained from J. Melamed, NYU School of Medicine. Tissue sections were stained as described previously (23) using antibodies against Art-27 (described in reference 23) (dilution, 1:250), URI (a rabbit polyclonal antibody from N. Djouder; dilution, 1:1,000), and AR (antibody N-20; dilution, 1:500; Santa Cruz Biotechnology).

For immunoblot analysis, cells were lysed in Triton buffer (50 mM HEPES [pH 7.5], 150 mM NaCl, 1 mM EDTA, 1 mM EGTA, 10% glycerol, 1% Triton X-100, 10 mM NaF, 25 μM $ZnCl_2$) and were supplemented with 1 mM phenylmethylsulfonyl fluoride (PMSF), 1 mM $NaVO_4$, 10 mg/ml of leupeptin, and 10 mg/ml of aprotinin. Protein lysates were quantified using Bio-Rad protein assay dye and were normalized for total protein concentration. Total protein was subjected to sodium dodecyl sulfate-polyacrylamide gel electrophoresis (SDS-PAGE) and was immunoblotted with antibodies against Art-27 (previously described in reference 22); AR (antibody 441) and ERK-1 (Santa Cruz Biotechnology); tubulin (Covance); hsp90 (BD Biosciences); p70S6 kinase (total), phosphorylated p70S6 kinase threonine 389, AKT (total), and phosphorylated AKT serine 473 (Cell Signaling); Brg1 (H-88; Santa Cruz); histone H3 (96C100; Cell Signaling); POLR2E (RPB5; Abcam); and URI (A301-164A-1; Bethyl). Protein bands were visualized using ECL Western blotting detection reagents (GE Healthcare). Protein expression levels were quantified using ImageJ software (version 1.42q; National Institutes of Health).

In immunoprecipitation experiments, cells were lysed as described above. Primary antibodies were added to 1.5 mg of total protein, and the mixture was incubated overnight at 4°C, followed by the addition of protein A/G agarose beads (Santa Cruz Biotechnology) for 2 h. For immunoprecipitation of URI, an antibody purchased from Abnova (H00008725-A01) was used. Immune complexes were washed extensively with Triton buffer and were solubilized using Laemmli sample buffer (Bio-Rad). Normal mouse IgG (Santa Cruz Biotechnology) or normal rabbit sera (Sigma-Aldrich) were used as controls.

Luciferase assay. HEK293 cells were seeded in a 24-well plate at a density of 1×10^5 per well. Cells were transfected with 0.2 μg ARR3 luciferase reporter, 0.05 μg of AR, increasing concentrations of pcDNA3-URI (0.05 μg, 0.1 μg, or 0.2 μg), and pCDNA3 (vector only) up to a total of 0.5 μg of DNA. Transfection was achieved using Lipofectamine reagent (Invitrogen). After transfection, the cells were allowed to recover in phenol red-free DMEM supplemented with 10% charcoal-stripped FBS (CFBS). Twenty-four hours posttransfection, cells either were left untreated or were treated with 10 nM R1881 (Perkin-Elmer) for an additional 24 h. Following treatment, cells were lysed in 1× reporter lysis buffer (Promega). Luciferase activity was quantified in a reaction mixture containing 25 mM glycine (pH 7.8), 10 mM $MgSO_4$, 1 mM ATP, 0.1 mg/ml bovine serum albumin (BSA), 1 mM dithiothreitol (DTT), and 1 mM D-luciferin (BD Biosciences) using a Lumat LB luminometer. Luciferase activity was normalized for protein content as calculated by the Bio-Rad protein assay.

ChIP assay. Chromatin immunoprecipitation (ChIP) was performed as described previously (22) with minor differences. Briefly, LNCaP cells stably expressing a nonsilencing shRNA (LNCaP-shNS) or an shRNA against URI (LNCaP-shURI) were grown in complete medium for 2 days in the presence of 1 μg/ml doxycycline to induce the expression of the shRNA. Proteins were double cross-linked with dithiobis(succinimidylproprionale) (DSP; Pierce) for 20 min and with 1% formalin for 10 min. Cells were lysed, and nuclei were collected, lysed in sonication buffer (1% SDS, 10 mM EDTA, 50 mM Tris-HCl [pH 8.0]), and sonicated for 12 min (30 s on, 30 s off) in a Bioruptor sonicator (model XL; Diagenode). Sonicated lysates were precleared for 2 h with protein A/G-agarose beads blocked with salmon sperm DNA (Millipore). Supernatants were then incubated overnight with a mixture of 2 μg anti-AR antibody 441 and 2 μg anti-AR antibody N-20, 5 μg of anti-Art-27 (23), or 4 μg of anti-RNA polymerase II (4H8; C-terminal domain [CTD] repeat antibody, ChIP grade; Abcam). Control ChIP was performed with normal mouse IgG and normal rabbit IgG sera. Immunocomplexes were then washed, and cross-linking was reversed. DNA was isolated with the Qiagen PCR purification kit, and quantitative PCR (Q-PCR) was performed using 1 to 5 μl of DNA. Relative enrichment was calculated as a percentage of 4% input normalized to IgG. The ChIP primers used for the NKX3.1 transcription start site (TSS) and upstream region (UPS) have been described previously (18). ChIP primers used for the NKX3.1 3′ untranslated region (3′ UTR) androgen response elements (AREs) have been described previously (25). The primers used for the experiments for which results are shown in Fig. 10 are as follows: P1F (TGCACTTCTAGGGCACATTG), P1R (GGATGCATGACTGTTTTTGG), P2F (GCTGTGCAAACATCATAGAGC), P2R (AGGAGCAATAGGGCATACCA), P2.5F (CTGATCAAACGTCACGATGC), P2.5R (GAGGAACAGCTGCTCTCATACA), P3F (GGCAGGACATCAAAATCACA), P3R (GCTTGTGTTTCCATCCCTCTA), P4F (GTCTCAGCACTTTGGGTGGT), P4R (AGTGCAGTGGAGAGATCATGG), P4.5F (TGTCTTTGGAGGACACTGGA), P4.5R (TTGGCAAAGCTGGTTTTCTT), P5F (AGCCGTCTTAGACCAGGACA), P5R (TAGATCCCACGCCATAAAGC), P6F (CAGTCACAGTACCGGTTGGA), P6R (TTTTAGGCCAGGACAAATGC), P7F (CCCCTGTAATTGGCTCTGAC), P7R (TGGGACGATCAAGACAAACA), P8F (ATCCCCAGGAGCTTCTCTCT), P8R (TAGGGGATTCCTTCCCCAGT), G1(TSS)F (GTCCTTCCTCATCCAGGACA), G1(TSS)R (CTGTCTCTGGCTGCTCGTG), I1F (GTGACAAAGCAGGGGTTGAC), I1R (CTTTACTGCCCACGGGATT), I2F (TCCGGAGAGCTCCTTAGTCA), I2R (GAACAAACAGCCCACTGTCA), G2F (CCGCAGAAGCGCTCCCGAGCT), G2R (CGAGGAGAGCTGCTTTCGCTT), U1F (AGGGGAGAGAGGGAAAATCA), U1R (ACACAGGAGGATGGAGTTGC), U2(AREI UTR)F (GATGGGTGGGAGGAGATGA), U2(AREI UTR)R (TGTCTTGGACAAGCGGAG), U3F (AGCCCGAGATCTGGTCTTTT), U3R (CAGAATCTGCCCCCAAACT), U4(AREII UTR)F (GGTTCTGCTGTTACGTTTG), U4(AREII UTR)R (CTTGCTTGCTCAGTGGAC), U5F (AACCATTTCACCCAGACAGC), U5R (CAGATTGGAGCAGGGTTTGT), UPSF (GGAGACCATTGCATGAACCT), and UPSR (AGAGCTGAGGGCTCTGAGTG).

Consecutive siRNA transient transfection. siGENOME SMARTpool small interfering RNAs (siRNAs) against URI or Art-27 and a control siRNA were purchased from Dharmacon. A total of 1.2×10^6 cells were plated in 6-cm-diameter plates and were transfected for 4 h with siRNAs and Lipofectamine 2000 on 2 consecutive days with an overnight recovery in a medium supplemented with 10% CFBS between the 1st and 2nd transfections and after the 2nd transfection. Recovery in a medium supplemented with 10% FBS was carried out for the experiment for which results are shown in Fig. 6a. Forty-eight hours after the 1st transfection, cells were treated according to the specific conditions described in the figure legend.

Q-PCR. Total RNA was isolated using the RNeasy kit (Qiagen, Inc.). Total RNA was reverse transcribed at 55°C for 1 h using Superscript III reverse transcriptase and oligo$(dT)_{20}$ primers (Invitrogen). Real-time PCR was performed using gene-specific primers (described in reference 18) and 2× SYBR

green *Taq*-ready mix (Sigma-Aldrich). Data were analyzed by the $\Delta\Delta C_T$ method using RPL19 as a control gene and were normalized to the values for control samples, which were arbitrarily set to 1.

Microarray analysis. URI was depleted in LNCaP cells using consecutive transient transfection of a control siRNA or a URI-directed siRNA, as described above. Forty-eight hours after the first transfection, cells were either left untreated or treated with 10 nM R1881 for 24 h. Total RNA was then isolated using the RNeasy kit (Qiagen, Inc.). Hybridization and analysis were performed at the Memorial Sloan-Kettering genomics core facility using the Affymetrix one-cycle protocol and HG_U133A 2.0 gene chips (Affymetrix). The expression of androgen-regulated genes was determined using RMAExpress software and the MultiExperiment Viewer (MeV), version 4.2, for statistical analysis. A 2-fold change threshold was used, and the NetAffx online tool was used to compare regulated genes in the Art-27 and URI knockdown experiments. Principal-component analysis (PCA) was performed using Agilent GeneSpring GX 10 software. PCA was performed for all experimental conditions with unfiltered gene contents. The three principal components representing the greatest variance in expression were plotted in a 3-dimensional gene expression space to visualize the general relationships among the different samples.

Soft-agar assay and neutral red growth assay. A total of 8.5×10^3 cells were resuspended in 1 ml of 0.35% agar and were layered on top of a previously prepared solid layer of 0.7% agarose (3 ml) in a 6-cm-diameter plate. Complete medium with or without 1 μg/ml doxycycline or with or without bicalutamide (BIC; Sigma-Aldrich) was added on top of the upper layer. The medium was changed every 2 days, and after 14 to 15 days, images of the colonies were taken using an inverted broad-field fluorescence microscope (Nikon Eclipse TE2000-E). Colonies in 10 random fields were counted, and the colony area was measured using ImageJ software. Statistical significance was calculated using the Wilcoxon signed-rank test. The neutral red growth assay was performed by plating 5×10^5 cells in 24-well plates. Neutral red dye was added directly to the medium to obtain a 2% final concentration. After 1 h, cells were washed in phosphate-buffered saline (PBS), and the dye was extracted with lysis buffer (50 mM Tris [pH 7.4], 150 mM NaCl, 5 mM DTT, 1% Triton X-100, 1% acetic acid). The absorbance of the solution at a λ of 540 nm was then measured.

Biochemical fractionation. Biochemical fractionation for the isolation of the chromatin-insoluble fraction P3 was performed as described in reference 31. Briefly, nuclei were lysed in a hypotonic buffer and were centrifuged to separate the nuclear soluble (S3), insoluble, and chromatin-enriched (P3) fractions. The P3 fraction was treated with 5 U of micrococcal nuclease (MNase) and was incubated at 37°C for the time indicated in Fig. 9a. The reaction was stopped with the addition of EGTA; the reaction mixture was then centrifuged at $1{,}700 \times g$ for 5 min, and Laemmli buffer was added to the supernatant.

λ phosphatase assay. The lambda phosphatase assay was carried out as described previously (11). Briefly cells were lysed in PL buffer (50 mM Tris-HCl [pH 7.5], 0.1 mM EDTA, 5 mM DTT, 250 mM NaCl, 0.5% NP-40) supplemented with protease inhibitors, and 200 μg of protein was used for the λ phosphatase assay. The reaction was carried out in λ phosphatase buffer in the presence of $MnCl_2$ and 400 U of λ phosphatase enzyme (New England Biolabs). The reaction mixture (total volume, 50 μl) was incubated for 5 min at 30°C, and the reaction was then terminated by adding 6× Laemmli buffer and boiling for 10 min at 95°C.

RESULTS

URI represses AR-mediated gene transcription. It has been reported that URI is a transcriptional repressor (8), and while URI mRNA expression is altered in prostatic intraepithelial neoplasia (PIN) and advanced prostate cancer (26), the role of URI in AR-mediated transcription is unknown. Therefore, to examine the putative role of URI in AR-mediated transcription, luciferase reporter gene assays were conducted using HEK293 cells transfected with FLAG-URI along with AR and an androgen-responsive ARR3-luciferase reporter. Cells were either left untreated or treated with the synthetic androgen R1881 for 24 h before luciferase measurement. The results show that expression of URI resulted in decreased AR-mediated transcription both in the absence and in the presence of R1881 (Fig. 1a).

To examine the impact of URI on endogenous gene transcription, the expression of two well-characterized androgen-regulated genes, those encoding prostate-specific antigen (PSA) and FKBP5, was evaluated in the presence or absence of URI protein. LNCaP cells were transfected with a control siRNA or an siRNA against URI and then were either left untreated or treated with R1881. Measurement of PSA and FKBP5 mRNAs via quantitative PCR (Q-PCR) analysis showed that knockdown of URI induced increases in PSA and FKBP5 mRNA transcription without affecting AR protein levels (Fig. 1b). These data indicate that URI acts as an AR repressor.

URI is required for repression of AR-mediated transcription by BIC. To determine if URI plays a role in gene repression mediated by AR antagonists, we investigated whether the loss of URI affected repression of the AR target genes PSA and FKBP5 by an AR antagonist (bicalutamide [BIC]). LNCaP cells were depleted of URI under conditions of hormone starvation (10% charcoal-stripped FBS [CFBS]) and then were either left untreated or treated with bicalutamide in complete medium supplemented with 10% FBS. FBS contains adequate endogenous steroids to activate AR, thus obviating the need to add exogenous androgens. Cells treated with medium supplemented with 10% CFBS after knockdown were used as a baseline for AR-mediated transcription analysis. The mRNA was isolated, and the expression of PSA and FKBP5 was measured by Q-PCR. As expected, bicalutamide treatment reduced androgen-mediated transcription of PSA and FKBP5 by 39.3% and 64.1%, respectively (Fig. 2a and b). Bicalutamide-mediated repression was alleviated in the presence of URI siRNA: PSA repression was reduced from 39.3% to 12.7% (Fig. 2a), and FKBP5 repression was reduced from 64.1% to 25.5% (Fig. 2b). This result indicates that URI, like Art-27 (18), is important in bicalutamide-mediated transcriptional repression of androgen-regulated genes.

URI inhibits LNCaP anchorage-independent growth. We next analyzed the growth of LNCaP cells either stably overexpressing URI or depleted of URI by stable shRNA targeting (Fig. 3a). These experiments did not reveal any differences in cell proliferation between control cells and cells with altered expression of URI when grown in monolayers. We speculated that URI might impact anchorage-independent growth, and we therefore performed experiments to assess the ability of cells overexpressing URI to grow in soft agar. Both control LNCaP cells harboring an empty vector and LNCaP-URI cells were cultured for 10 to 15 days in soft agar. The numbers and areas of colonies were then measured. While overexpression of URI did not change the number of colonies (Fig. 3c), the colonies formed by the LNCaP-URI cells were smaller ($P < 0.0001$) than those formed by control LNCaP cells (Fig. 3d). This suggests that URI overexpression diminishes the ability to grow under anchorage-independent conditions as measured by colony formation in agar but does not directly affect cell growth.

To determine if URI also affects bicalutamide repression of prostate cancer cell growth, soft-agar colony assays were performed in the presence or absence of BIC. As expected, bicalutamide strongly inhibited individual colony growth in control LNCaP cells (LNCaP-vector [Fig. 3e] and LNCaP-shNS [Fig. 3f]). Overexpression of URI further inhibited cell growth in soft agar in the presence of BIC (0.078 ± 0.003 versus

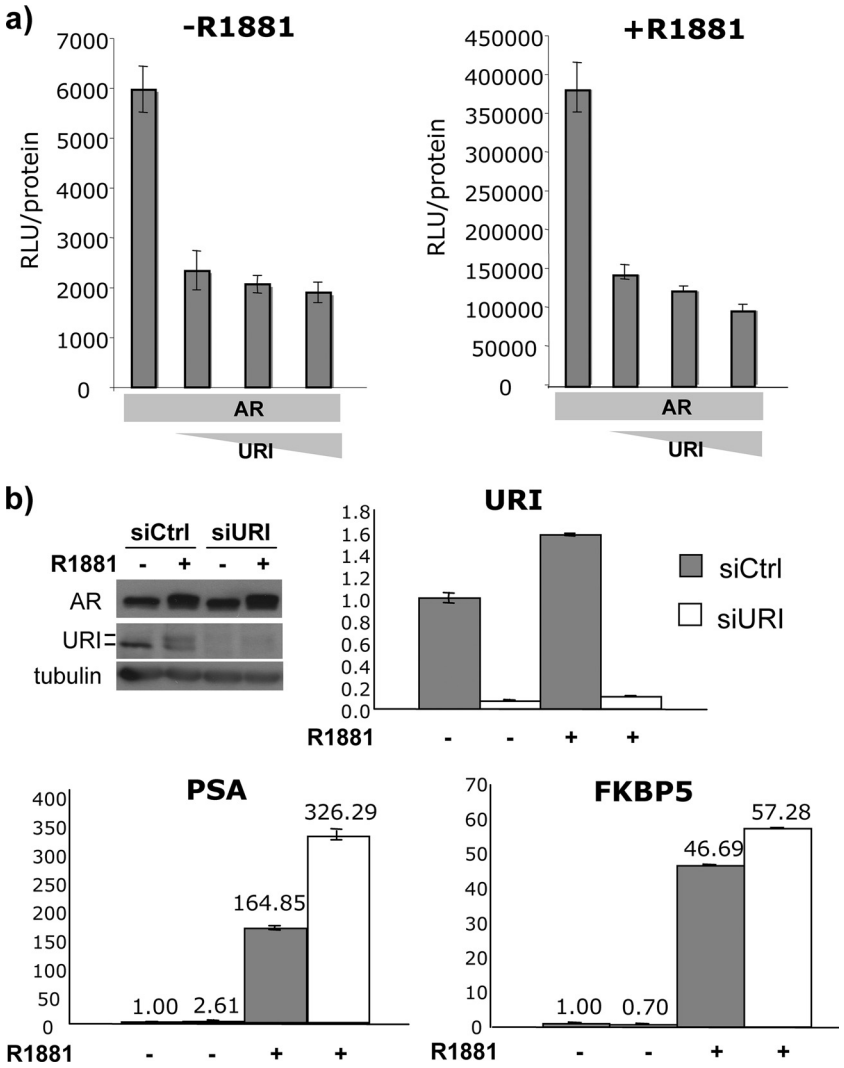

FIG. 1. URI represses androgen receptor-mediated transcription. (a) HEK293 cells were transfected with FLAG-URI together with AR and an ARR3-luciferase reporter construct. Twenty-four hours posttransfection, cells were either left untreated (left) or treated with 10 nM R1881 (right) for 24 h. The experiment was conducted in triplicate. Error bars represent standard deviations. (b) URI was depleted in LNCaP cells using an siRNA against URI (siURI) or a control siRNA (siCtrl) as described in Materials and Methods. After knockdown, cells either were left untreated or were treated with 10 nM R1881 for 24 h. (Top left) Horizontal lines on the left indicate the two bands of URI protein. URI and AR proteins were analyzed by Western blotting, and tubulin was used as a loading control. (Top right and bottom) The relative mRNA levels of URI, PSA, and FKBP5 were quantified by Q-PCR using specific primers. Values were normalized to the values for RPL19 mRNA.

0.039 ± 0.007 relative unit [Fig. 3e]). Moreover, knockdown of URI in LNCaP-shURI cells grown in the presence of BIC alleviated bicalutamide repression (0.07 ± 0.005 versus 0.1 ± 0.011 relative unit [Fig. 3f]). These findings further indicate an important role for URI in bicalutamide action.

Taken together, these results suggest that URI acts like a putative tumor suppressor to repress AR-mediated gene transcription and to inhibit anchorage-independent growth. URI probably does not have a direct role in cell cycle regulation, because its overexpression or depletion does not affect the growth of adherent LNCaP cells. However, the changes induced by URI overexpression or depletion confer a disadvantage or advantage, respectively, for the anchorage-independent growth of prostate cancer cells.

URI is phosphorylated in response to androgen downstream of mToR. URI was previously shown to be phosphorylated in response to several stimuli downstream of the mTOR pathway (7, 11). Furthermore, in prostate cells, the mToR pathway is activated by androgen treatment following AR transcriptional activation (32). To determine if URI expression or modification is affected by androgen treatment, we treated the prostate cancer cell line LNCaP with increasing concentrations of the synthetic hormone R1881 for 24 h. Western blot analysis indicates that URI appears as a single band in the absence of the hormone. Following hormone treatment, a URI band with slower electrophoretic mobility appears, and URI can be visualized by Western blotting as a double band. Moreover, expression of the upper band of URI is increased in a hormone-dependent manner (Fig.

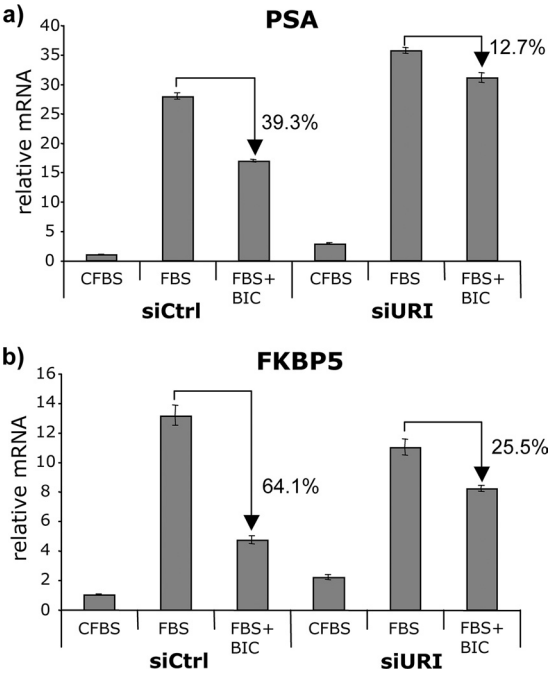

FIG. 2. URI affects the response to bicalutamide. LNCaP cells were treated with a control siRNA (siCtrl) or with an siRNA against URI (siURI) as described in Materials and Methods. After knockdown was performed in 10% CFBS, cells were treated for an additional 24 h with a medium containing either 10% CFBS, 10% FBS, or 10% FBS plus bicalutamide (10 mM). mRNA was then isolated, and the relative levels of PSA (a) and FKBP5 (b) mRNAs were measured and normalized to RPL19 mRNA levels.

4a), suggesting that URI is modified in response to a pathway activated downstream of AR.

Given our interest in the role of URI in the nucleus, we evaluated whether hormone-dependent phosphorylated URI was present in the nucleus versus the cytoplasm of LNCaP cells. Nuclear/cytoplasmic fractionation was performed in LNCaP cells treated with 10 nM R1881 for 24 h. The results indicate that the phosphorylated form of URI is present in both cellular compartments (Fig. 4c). λ phosphatase assays using LNCaP cell lysates treated for 24 h with 10 nM R1881 confirmed that the hormone-dependent upper band of URI was due to phosphorylation (Fig. 4b).

It has been reported that in the mitochondria, URI is phosphorylated by p70S6 kinase downstream of mToR (7). To determine if androgen-mediated URI phosphorylation is mToR dependent, LNCaP cells were treated with increasing concentrations of R1881 in the presence or absence of rapamycin, a known mToR inhibitor. In the presence of rapamycin, the hormone-dependent upper band of URI was completely inhibited, suggesting mToR-dependent phosphorylation of URI. mToR-dependent phosphorylation of p70S6K on threonine 389 is shown to confirm inhibition/activation of the mToR pathway (Fig. 4a).

Previous studies have linked mToR with Akt activation in prostate cancer (17, 21), and it is well established that in a high percentage of prostate cancers, PTEN phosphatase is mutated or deleted. In these tumors, aberrant PTEN expression results in hyperactivation of Akt. Therefore, to determine if hormone-dependent URI phosphorylation is affected by Akt inhibition, we either left LNCaP cells (which have constitutively active Akt because of a mutated PTEN) untreated or treated them with 10 nM R1881 for 24 h in the presence or absence of Akt inhibitor VIII. URI phosphorylation was completely inhibited in the presence of the Akt inhibitor (Fig. 4d), and the phosphorylation of p70S6K was also greatly diminished.

The observation that URI protein is phosphorylated downstream of the mToR pathway suggests that URI phosphorylation could integrate extracellular and metabolic stimuli with transcriptional regulation by the androgen receptor.

URI binds Art-27 in prostate cells. URI was identified as an Art-27 binding partner in an immunoprecipitation and mass spectrometry experiment conducted in HeLa cells (11). Art-27 is a well-established AR corepressor whose nuclear expression correlates with decreased prostate cancer recurrence (18). To determine if the effect of URI on AR-dependent transcription was mediated by Art-27, we initially asked if URI and Art-27 were in a complex in prostate cells. Immunoprecipitation experiments were performed using whole-cell lysates from the prostate cancer cell lines LNCaP, LAPC4 (data not shown), and PC3. In all cell lines analyzed, URI coimmunoprecipitated with Art-27, and vice versa (Fig. 5a and b). Coimmunoprecipitation experiments with cytoplasmic and nuclear fractions were also performed, verifying that URI interacts with Art-27 in both cellular compartments (data not shown). URI also immunoprecipitated with Art-27 in PC3 cell lines that do not express AR protein, indicating that the URI–Art-27 interaction can be AR independent (Fig. 5b). Although an interaction of Art-27 with AR was observed previously (16), we were not able to coimmunoprecipitate AR with URI (Fig. 5a, right). These results may indicate either that there is an Art-27/AR complex that does not include URI or, more likely, that our anti-URI antibody cannot recognize URI in complex. Alternatively, the URI–Art-27–AR complex may be present in low abundance, may be transient, or may not be preserved under conditions of cell lysis and immunoprecipitation.

To verify that URI and Art-27 were expressed in the same cells *in vivo* and therefore are potentially part of a protein complex in human prostate cells, we analyzed the expression of URI, Art-27, and AR in consecutive sections of human prostate tissues, using a polyclonal antibody that specifically recognizes URI protein, as indicated by a diminished signal on a Western blot for cells depleted of URI by shRNA (Fig. 5c). *In vivo* staining showed that URI, Art-27, and AR were expressed in prostate epithelial cells (Fig. 5d), with only negligible URI and Art-27 expression in the stroma, as previously reported (23). These observations indicate that AR, URI, and the AR cofactor Art-27 are colocalized in prostate epithelial cells.

URI affects Art-27 protein stability. The fact that Art-27 and URI are coimmunoprecipitated from prostate cell protein extracts (Fig. 5) suggests that they are in complex *in vivo*. To determine if the loss of one component of the complex affects the other, protein levels of URI or Art-27 were selectively diminished in LNCaP cells using transient transfection of siRNA pools directed against one of the two proteins. A nonspecific siRNA was used as a control. The results indicate that specific depletion of Art-27 protein correlated with loss of URI protein and that depletion of URI protein correlated with loss of Art-27 (Fig. 6a and b). Interestingly, we observed that the

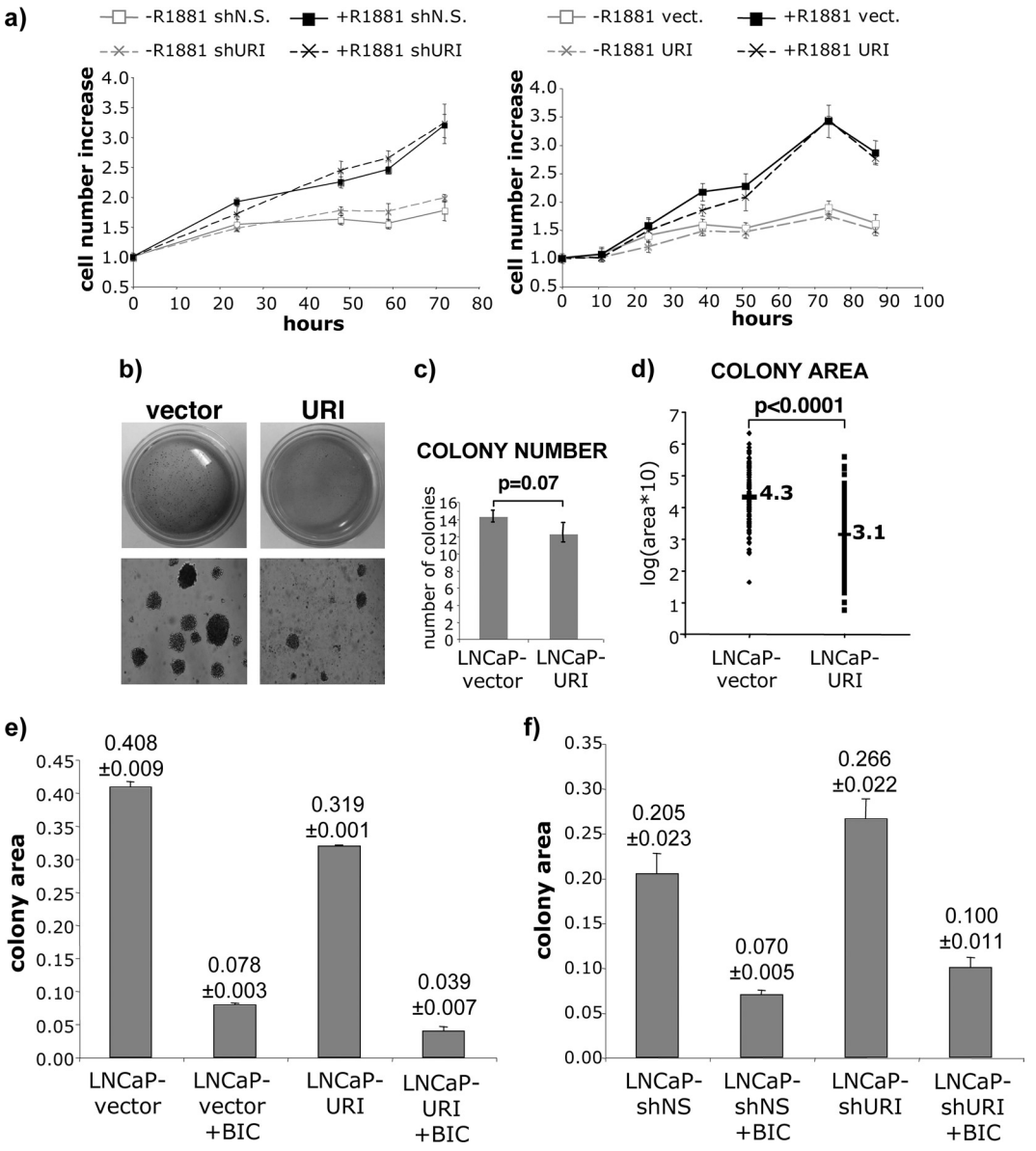

FIG. 3. URI inhibits LNCaP anchorage-independent growth. (a) Growth curves of LNCaP cells depleted of URI (left) or overexpressing URI (right). LNCaP stable cell lines were cultured in hormone-starved medium (−R1881) or in the presence of 0.1 nM R1881 (+R1881). The number of cells was measured by neutral red uptake. Each time point was normalized for the initial number of cells at time zero. (b) LNCaP cells stably overexpressing an empty vector (LNCaP-vector) or URI (LNCaP-URI) were grown in soft agar for 15 days as described in Materials and Methods. Representative colonies are shown. (c) The number of colonies was counted in 10 random fields. (d) The areas of 200 colonies for each condition were measured. The area is reported on a logarithmic scale, and the geometrical mean is indicated. Statistical analysis was performed using the Wilcoxon test for colony area and the Student *t* test for colony number. (e and f) LNCaP-vector and LNCaP-URI or LNCaP cells stably expressing a control shRNA (LNCaP-shNS) or an shRNA against URI (LNCaP-shURI) were grown in the presence or absence of bicalutamide (10 mM) for 15 days in soft agar. The areas of 200 colonies from each treatment were measured. All differences between colony areas were statistically significant ($P < 0.0001$). The results shown are representative of 3 independent experiments carried out in triplicate.

band of unmodified URI (the lower band) was preferentially decreased (Fig. 6a) upon Art-27 depletion. This suggests that the phosphorylated form of URI might be part of a more stable complex. Moreover, Q-PCR analysis revealed that Art-27 degradation upon URI depletion is due to a posttranscriptional event, because Art-27 mRNA was not affected by URI depletion (Fig. 6d). Consistent with these results, stable overexpression of URI in either HEK293 (Fig. 6c) or LNCaP (Fig. 6f) cells resulted in stabilization of Art-27 protein without affecting Art-27 mRNA (Fig. 6e).

To understand the effect of modulation of URI protein on Art-27 protein levels, we treated cells with cycloheximide (CHX) to block protein translation. Stable LNCaP cell lines overexpressing URI (LNCaP-URI), with LNCaP cells expressing an empty vector (LNCaP-vect) as a control, or depleted of URI (LNCaP-shURI), with LNCaP-shNS as a control, were

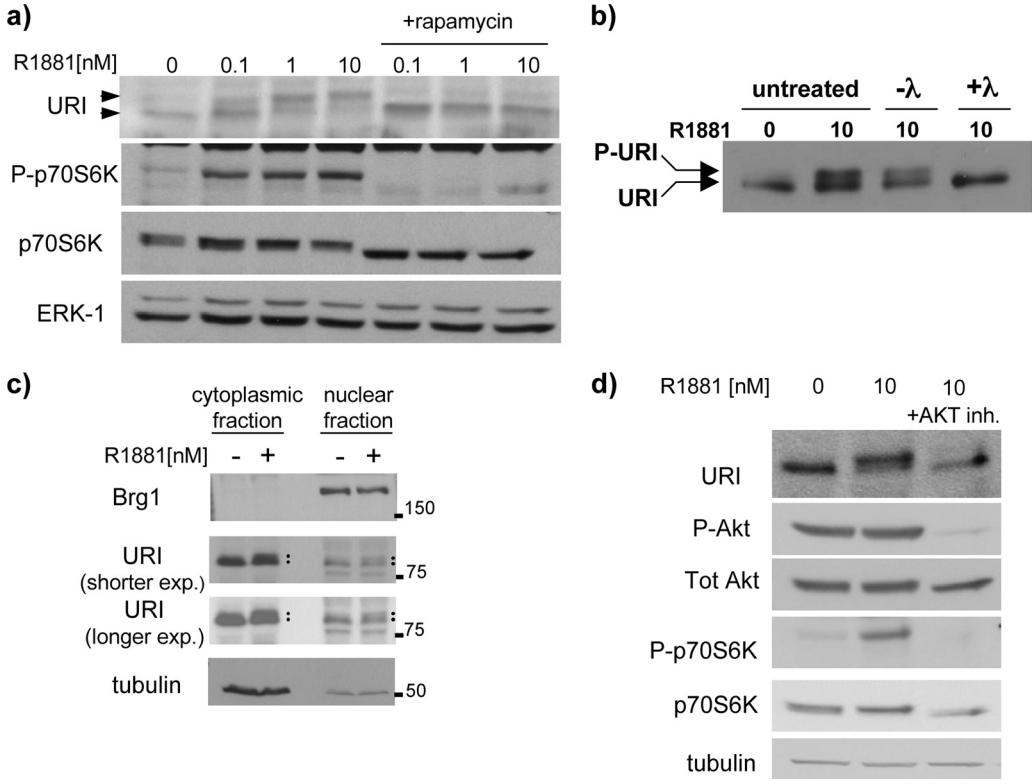

FIG. 4. Hormone treatment results in URI phosphorylation downstream of mToR. (a) LNCaP cells were starved in 10% CFBS overnight and were then treated for 24 h either with ethanol (0 nM R1881) or with increasing concentrations of R1881 in the presence or absence of rapamycin (100 nM). Whole-cell lysates were analyzed by Western blotting for the indicated proteins. ERK-1 protein was used as a loading control. The arrowheads indicate the two bands of URI. (b) Lambda phosphatase assay. LNCaP cells were treated as described in the legend to panel a (untreated). Part of the lysate from cells treated with 10 nM R1881 was treated with λ phosphatase (+λ) or not treated (−λ) as described in Materials and Methods. (c) Nuclear and cytoplasmic fractions were prepared from LNCaP cells that were either left untreated or treated with 10 nM R1881 for 24 h. Brg1 and tubulin were used as nuclear and cytoplasmic markers, respectively. Dots on the URI blots indicate the two bands of URI. exp., exposure. (d) LNCaP cells were cultured as described for panel a in the presence or absence of 20 μM Akt inhibitor VIII (inh.).

used (Fig. 6i). Cells were lysed at the time points indicated in Fig. 6f through h, and the Art-27 protein level was analyzed by Western blotting (Fig. 6f to h). As in the preceding experiments, the amount of Art-27 protein was increased in URI-overexpressing LNCaP cells and was decreased in URI knockdown cells (compare Fig. 6f and g for the same exposure times). In control cells (LNCaP-shNS and LNCaP-vect), the half-life of Art-27 was longer than 8 h, and we were unable to detect any protein loss after 8 h of CHX treatment. However, upon the loss of URI, Art-27 protein had a half-life of about 6.5 h (Fig. 6h). The same analysis was performed for AR. In both control cells and LNCaP cells overexpressing or lacking URI, AR had a half-life of about 6 h (data not shown), suggesting that URI has no effect on AR protein stability. Therefore, changing the stoichiometry of either URI or Art-27 protein results in altered levels of the other, supporting the hypothesis that URI and Art-27 are in complex.

Diminution of URI protein levels results in decreased Art-27 and increased AR occupancy on the NKX3.1 gene. Overall, our studies suggest that URI and Art-27 act in concert to regulate gene transcription. Since previous ChIP analyses indicated that Art-27 is recruited to the NKX3.1 gene (18), we tested whether Art-27 and URI functionally interact at NKX3.1 regulatory sites. ChIP analysis was performed in LNCaP cells stably expressing a nonsilencing shRNA (LNCaP-shNS) or an shRNA against URI (LNCaP-shURI). NKX3.1 was specifically examined because we observed highly reproducible recruitment of Art-27 on a region close to the transcription start site (TSS). The results show that a decrease in URI protein levels results in a decrease of Art-27 occupancy on the NKX3.1 gene, consistent with the idea that loss of URI depletes the pool of Art-27 directly involved in transcription regulation (Fig. 7a).

Since NKX3.1 is an AR-regulated gene, we also investigated whether URI knockdown affected AR recruitment on the known AREs in the 3′ untranslated region (3′ UTR) of NKX3.1 (25). Interestingly, upon URI knockdown, we observed an increase of AR recruitment at both AREI and AREII in the 3′ UTR of NKX3.1, suggesting a direct role of URI in AR transcription regulation (Fig. 7b). Further, enhanced AR recruitment likely explains the increase in NKX3.1 mRNA levels observed in response to URI knockdown (Fig. 7c).

URI and Art-27 have similar effects on AR-mediated gene transcription. In order to understand the broader role of URI in AR-mediated gene transcription, we performed genome-wide expression profiling to identify genes affected by decreased levels of URI protein using DNA microarray technology. mRNAs were isolated from LNCaP cells depleted of URI

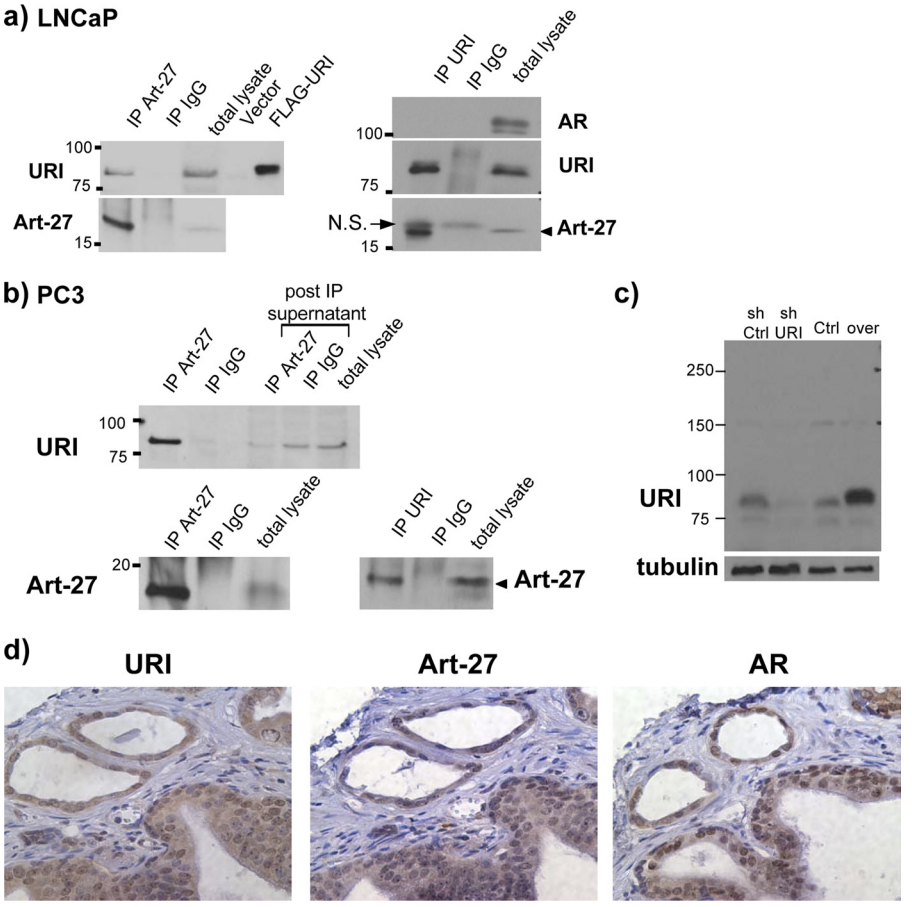

FIG. 5. URI interacts with Art-27 in prostate cells. (a and b) LNCaP (a) or PC3 (b) cells were cultured in complete medium. Whole-cell lysates were incubated with an antibody against Art-27 or URI or with a control antibody against normal rabbit IgG (for Art-27) or normal mouse IgG (for URI). Immunocomplexes were precipitated and were analyzed by SDS-PAGE, and membranes were probed with the indicated antibodies. The arrow indicates a nonspecific (N.S.) band, and the arrowheads indicate Art-27 protein. IP, immunoprecipitation. (c) Validation of the polyclonal anti-URI antibody used for tissue staining. Western blot analysis was performed on lysates from cells expressing either a control shRNA (shCtrl), an shRNA against URI (shURI), an empty vector (Ctrl), or FLAG-URI (over). (d) Consecutive sections of human prostate tissues were immunostained with antibodies against URI, Art-27, or AR to show the colocalization of the three proteins in prostate epithelial cells. Positive immunoreactivity appears brown, and cells that are not stained appear blue due to hematoxylin.

and were treated in the same way as in the previously published analysis of genes affected by Art-27 knockdown (18). LNCaP cells were treated with a control siRNA or an siRNA against URI, with or without 10 nM R1881, for 24 h. mRNAs were isolated and hybridized to the HG_U133.2 Affymetrix chip. Each knockdown was performed in duplicate. Androgen-dependent genes obtained from the Art-27 and URI knockdown experiments were compared (Fig. 8a). Most genes responded in the same way to hormone treatment in the control cells, indicating good reproducibility between the two sets of experiments. In line with our finding that URI and Art-27 proteins are tightly dependent on one another, we observed substantial overlap of androgen-dependent genes in cells depleted of Art-27 and cells depleted of URI. Interestingly, when we compared overlapping probes, 30 and 49 probes were up- or downregulated, respectively, by hormone only upon URI or Art-27 depletion, suggesting that these genes become hormone dependent in the absence of Art-27 or URI. Additionally, 83 and 28 probes were up- or downregulated, respectively, by hormone only in control cells, suggesting that Art-27 and URI are essential for the hormone responsiveness of these genes. Principal-component analysis shows that URI knockdown and Art-27 knockdown have similar effects on gene expression; samples depleted of URI or Art-27 and treated with hormone cluster together, apart from their respective controls (Fig. 8b).

We previously demonstrated that Art-27 depletion has an effect on a subset of genes involved in DNA damage response and cell proliferation (namely, CCNA2, TTK, BRIP1, GTSE1, CDC6, BUB1, CHK1, ATR, and HUS1) (18). We therefore measured the expression of these genes upon URI depletion (Fig. 8c). Q-PCR analysis showed that URI knockdown affects the expression of most of these genes in a manner similar to that of Art-27 knockdown, again suggesting that URI and Art-27 interact not only physically but also functionally. Interestingly, the expression of DNA damage-related genes CHK1 and HUS1 did not change upon URI knockdown, while ATR expression was inhibited by URI depletion. The transcription of these DNA damage-related genes, in contrast, was shown to be upregulated upon Art-27 knockdown (18), possibly suggesting URI- and Art-27-specific functions (Fig. 8c). Collectively,

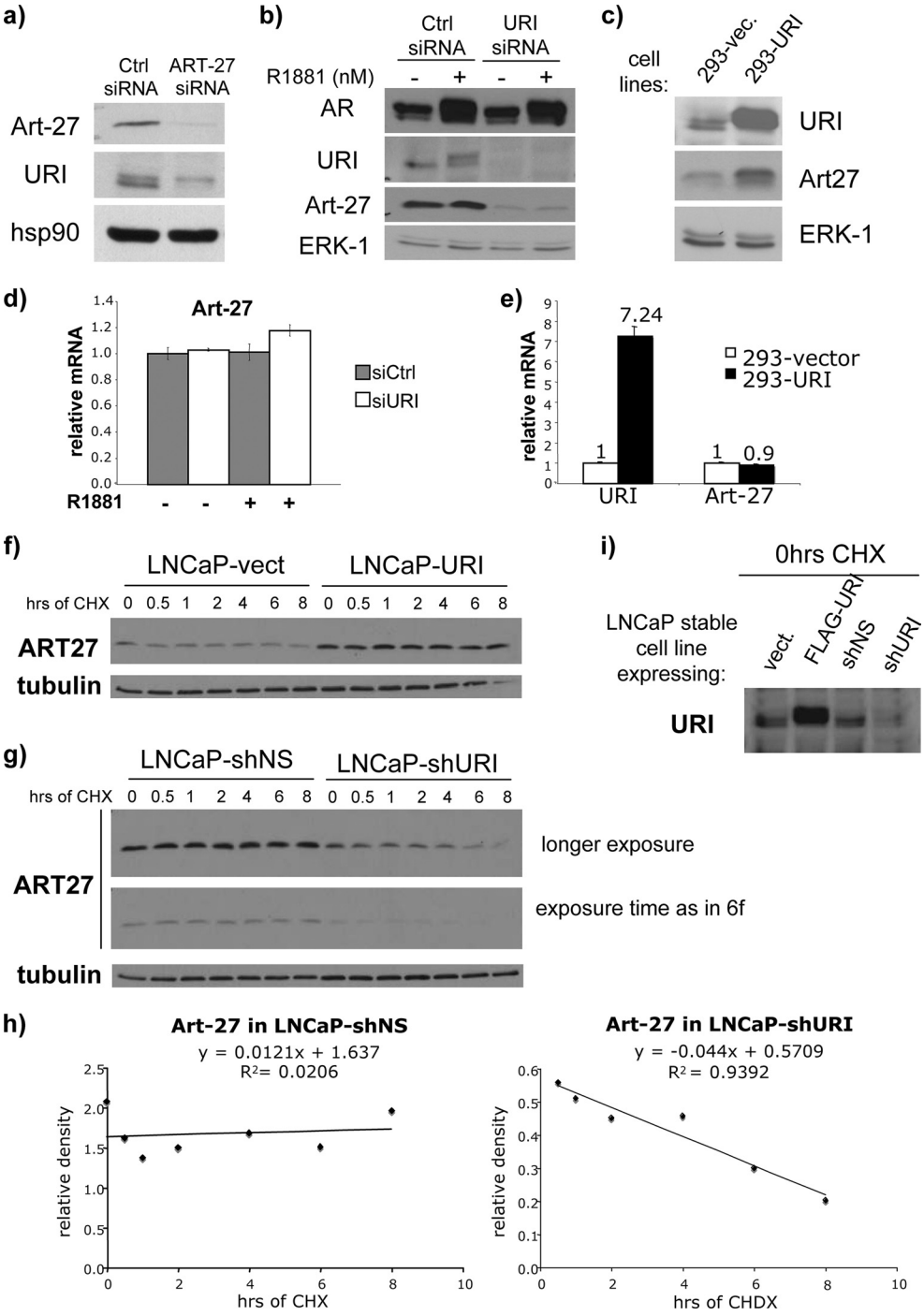

FIG. 6. URI and Art-27 affect each other's stability. (a) Art-27 was depleted from LNCaP cells grown in a medium supplemented with 10% FBS as described in Materials and Methods, using either a control (Ctrl) siRNA or an siRNA against Art-27. The indicated proteins were analyzed by Western blotting. hsp90 protein was used as a loading control. (b) LNCaP cells were depleted of URI using an siRNA against URI (URI siRNA). Cells were then either left untreated or treated with 10 nM R1881 for 24 h. AR, URI, and Art-27 protein levels were analyzed by Western blotting. (c) 293 cells stably overexpressing an empty vector (293-vec.) or a FLAG-URI construct (293-URI) were lysed, and Art-27 and URI protein levels were analyzed by Western blotting. ERK-1 protein was used as a loading control. (d and e) LNCaP cells (d) were treated as described for panel b, and stable 293 cell lines (e) were treated as described for panel c. mRNA was isolated, and URI and Art-27 mRNAs were quantified by Q-PCR. All values were normalized to those for RPL19 mRNA. (f and g) LNCaP cells stably overexpressing either an empty vector (LNCaP-vect), URI (LNCaP-URI), a control shRNA (LNCaP-shNS), or an shRNA against URI (LNCaP-shURI) were treated for the indicated times with 25 μM cycloheximide (CHX). Cells were lysed, and equal amounts of protein from each sample were loaded on a polyacrylamide gel. Tubulin (used as a loading control) and Art-27 proteins were analyzed by Western blotting. (h) Graphs showing densitometry analysis of Art-27 bands for LNCaP-shNS and LNCaP-shURI cells. (i) URI protein levels at the beginning of the experiment (0 h CHX) were also analyzed by Western blotting to verify the overexpression or depletion of URI.

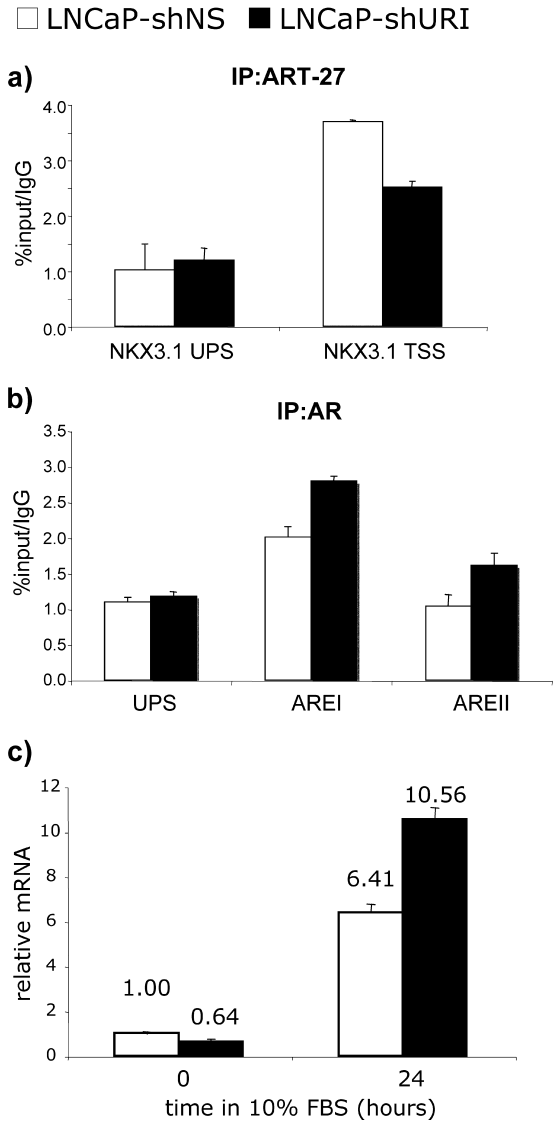

FIG. 7. URI loss decreases Art-27 and increases AR recruitment on chromatin. ChIP was performed as described in Materials and Methods. (a) Art-27 recruitment on a control NKX3.1 upstream region (UPS) and on a region of NKX3.1 close to the transcription start site (TSS). (b) AR recruitment on the NKX3.1 UPS and on AREI and AREII in the 3′ untranslated region of NKX3.1. The results are expressed as percentages of input normalized for IgG recruitment. (c) Q-PCR analysis of NKX3.1 transcripts after serum starvation for 18 h (0 h in 10% FBS) and 24 h of 10% FBS treatment. (Cells were treated with 1 μg/ml doxycycline throughout the experiment to induce shRNA expression.)

these results show a strong interdependence between Art-27 and URI, and they suggest that Art-27 and URI act in concert to regulate gene transcription.

The URI/Art-27 protein complex binds chromatin independently of AR. The results presented above indicate that URI may affect AR transcription through the stabilization of the AR corepressor Art-27. We also showed that loss of URI impacts AR recruitment to a target gene. One possible explanation for the increased AR recruitment on DNA in cells depleted of URI is that an URI-containing complex binds and possibly modifies chromatin. To determine if URI binds chromatin, we isolated the cytoplasmic and nuclear soluble fractions (S2 and S3, respectively) and the nuclear insoluble fraction (P3) from LNCaP cells grown in complete medium (31). The P3 fraction, which contains DNA and proteins tightly bound to chromatin, was then treated with micrococcal nuclease (MNase) for the times indicated in Fig. 9a to release chromatin-bound proteins into the soluble fraction. Western blot analysis showed that URI and Art-27 are bound to chromatin and that, after treatment with MNase, URI and Art-27 pass from the insoluble to the soluble fraction (Fig. 9a). Tubulin was used as a control to ensure the complete absence of the cytoplasmic fraction in the P3 fraction. Histone H3 was found to be present in the soluble P3 fraction before MNase treatment (0 min of MNase treatment), and its level increased with subsequent nuclease treatment. As expected, AR, RPB5, and RPB1 (the largest subunit of RNA polymerase II) are also bound to chromatin from LNCaP cells cultured in complete medium.

To determine if the chromatin-bound URI is in complex with Art-27, the P3 fraction was isolated from LNCaP cells and was treated with MNase. Art-27 was then immunoprecipitated from the MNase-treated P3 fraction. Western blot analysis revealed that URI coimmunoprecipitates with Art-27 (Fig. 9b) from the MNase-treated nuclear fraction, suggesting that URI binds to Art-27 on chromatin. We also found that a small fraction of AR binds Art-27 on chromatin, as expected from the previously observed interaction of Art-27 with AR, and in line with the established role of Art-27 as an AR corepressor.

The experiments described above examine the interaction of URI, Art-27, and AR under normal, nonsynchronized growth conditions. To understand the behavior of these proteins in response to hormone treatment, the same biochemical fractionation scheme was performed using hormone-starved LNCaP cells or cells treated for 24 h with the synthetic androgen R1881 (10 nM). As expected, AR was completely absent in the chromatin fraction of hormone-starved cells but was bound to the DNA in LNCaP cells treated with R1881. Surprisingly, URI and Art-27 were bound to chromatin both in the presence and in the absence of the hormone (Fig. 9c), suggesting that a fraction of URI and Art-27, probably in complex with one another, binds chromatin independently of the AR.

To confirm that Art-27 and URI are already on the chromatin before AR recruitment, specifically on the NKX3.1 gene, we performed ChIP assays in the presence or absence of the hormone (Fig. 9d). Consistent with the fact that URI and Art-27 bind chromatin in an androgen-independent manner, analysis of AR and Art-27 at the NKX3.1 TSS shows that, while AR is recruited in response to dihydrotestosterone (DHT), Art-27 is present at the TSS in the presence and absence of hormone. Taken together, our results suggest that the Art-27/URI complex is present at sites of AR binding within the NKX3.1 gene prior to the recruitment of AR.

These results, together with the previously reported binding of URI and Art-27 to the helicases TIP49 and TIP48 and to RNA pol II (3, 11), support the hypothesis that Art-27 and URI bind DNA prior to the recruitment of AR, perhaps modifying chromatin structure.

Art-27 recruitment on the NKX3.1 gene. To gain a better understanding of the role of the Art-27/URI complex in gene

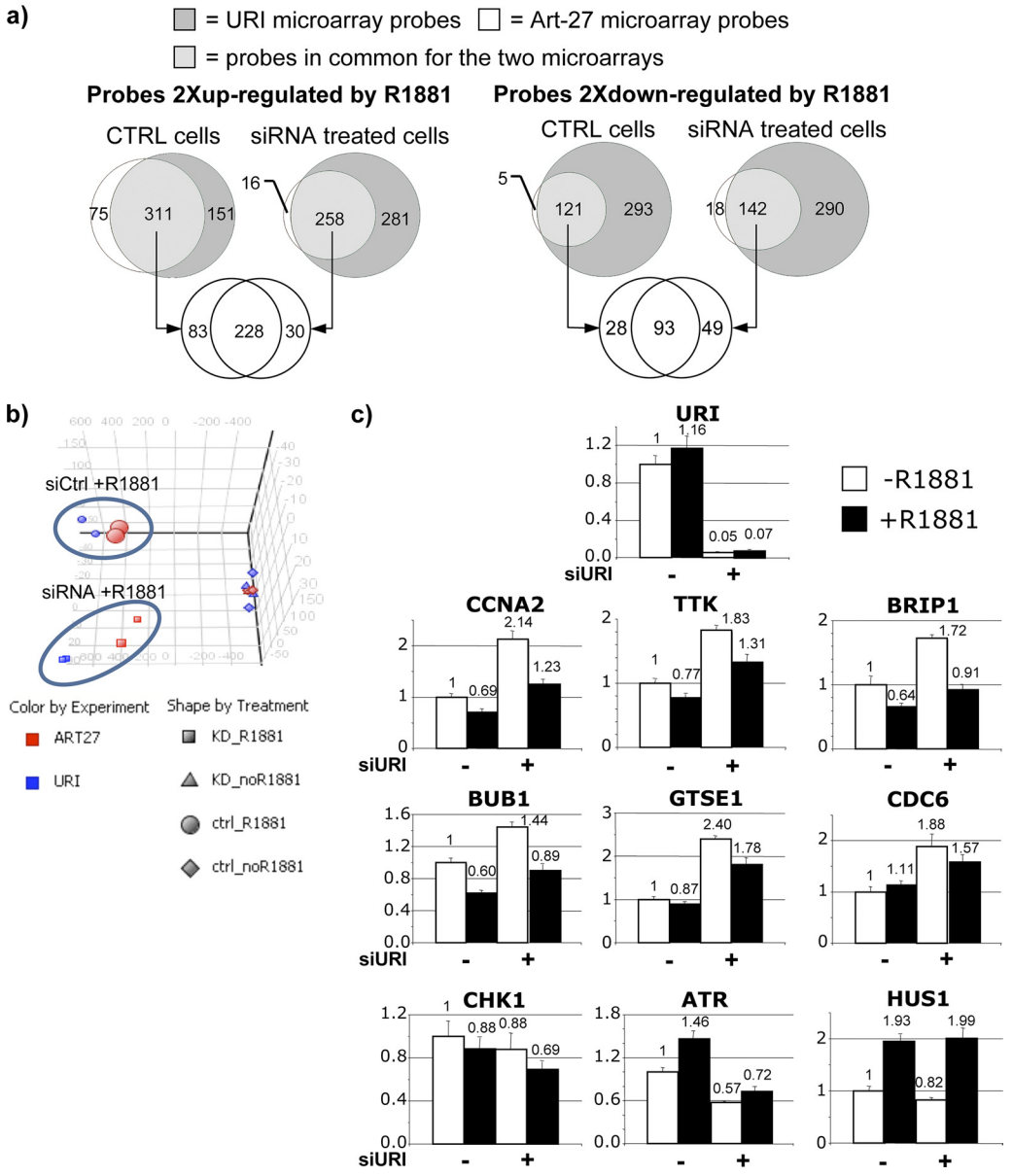

FIG. 8. URI loss affects AR transcription similarly to Art-27 loss. LNCaP cells were depleted of URI or Art-27 and were analyzed as described in Materials and Methods. (a) The Venn diagrams show the numbers of probes up- or downregulated after R1881 treatment in the two microarrays for Art-27 and URI knockdown. Overlapping areas in light gray are proportional to the number of probes in common between the two microarrays. (b) The three principal components with the greatest variance for the gene expression profiles of the Art-27 and URI microarrays were plotted in a 3-dimensional space using PCA. KD, knockdown. (c) LNCaP cells were treated with an siRNA against URI (+siURI) or a control siRNA (−siURI) as described in Materials and Methods. The expression of a subset of genes previously shown to be affected by Art-27 knockdown (18) was analyzed by Q-PCR. The relative amount of mRNA is reported for each bar.

transcription, we investigated the recruitment of Art-27 along the entire NKX3.1 gene using a ChIP assay. We immunoprecipitated AR, Art-27, and RNA polymerase II. Because we were not able to immunoprecipitate URI in the ChIP assay with multiple antibodies from a variety of sources, we hypothesize that URI is likely buried within a large multiprotein complex in which the antibody epitopes are masked. However, our data suggest that URI is recruited on the DNA together with Art-27 (Fig. 9b), and therefore, recruitment of one protein is likely to reflect recruitment of the other. In line with this idea, Art-27 has two peaks of recruitment on the NKX3.1 gene (Fig. 10): a major peak on the TSS and a second, smaller peak on the known AREI enhancer region in the 3′ UTR of NKX3.1. Finding Art-27 at the TSS is predicted based on interaction with URI, a known interactor with the RPB5 subunit of polymerases. In addition, the presence of Art-27 at the AREI supports our previous finding indicating that Art-27 interacts with AR (16). As expected, AR is strongly recruited on the 3′ UTR AREI region, and pol II is present on the body of the gene, with a stronger peak of recruitment

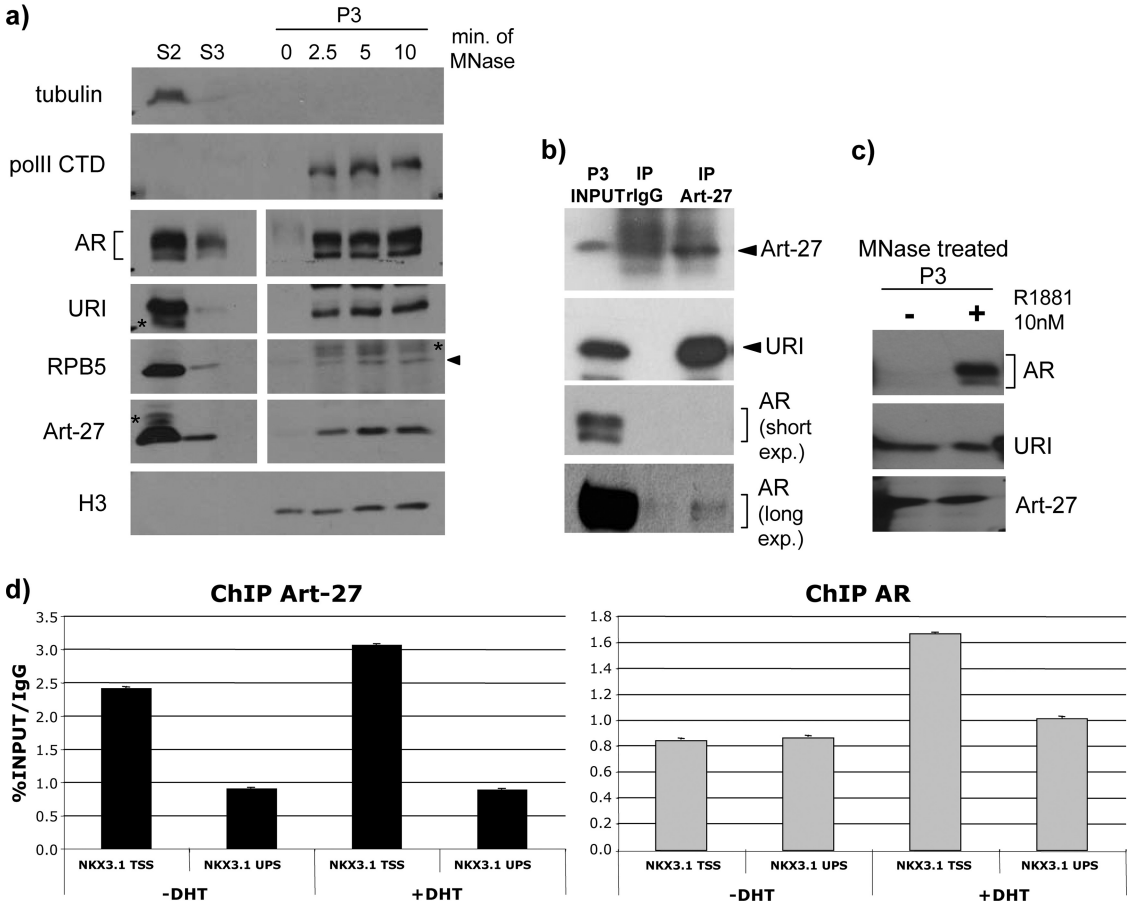

FIG. 9. URI and Art-27 bind to chromatin in an androgen-independent manner. (a) Western blotting of fraction P3 treated with micrococcal nuclease (MNase) for the indicated times. The cytoplasmic soluble fraction (S2), nuclear soluble fraction (S3), and nuclear insoluble fraction (P3) were isolated from LNCaP cells growing in complete medium. Asterisks indicate nonspecific bands, and the arrowhead indicates the protein of interest. (b) Fraction P3 treated with MNase (P3 INPUT) was used to immunoprecipitate (IP) Art-27 with specific rabbit antibodies against Art-27 or control rabbit antibodies (rIgG). A longer exposure (exp.) of the AR blot is presented to show the small fraction of AR immunoprecipitated with Art-27. (c) LNCaP cells were hormone starved for 24 h and were then either left untreated or treated for an additional day with R1881 (10 nM). The AR, URI, and Art-27 proteins from the P3 fractions treated with MNase were analyzed by Western blotting. (d) ChIP of Art-27 (left) and AR (right) after 3 days of hormone starvation followed by 4 h of treatment with 10 nM DHT (or no treatment [−DHT]). All the results are expressed as the percentage of input normalized for IgG recruitment.

on the TSS of NKX3.1. Collectively these results show that Art-27, probably in complex with URI, is recruited on the NKX3.1 TSS and ARE.

DISCUSSION

In this study we identify URI, an RPB5-interacting protein, as a new protein involved in controlling androgen receptor transcription. We demonstrate that URI is part of a complex containing the previously identified AR corepressor Art-27. URI and Art-27 are characterized by domains that share high homology with the alpha subunits of prefoldin. Prefoldin is a heterohexameric chaperone that is known to be involved in the presentation of unfolded target proteins to the cytosolic chaperonins (c-cpn; also called CCT or TRiC) (29). Despite this structural homology, we did not observe chaperone activity for Art-27 or URI. We ruled out the possibility that URI is itself a target protein for facilitated folding by c-cpn/CCT/TRiC by using an *in vitro* binding assay of URI to CCT (data not shown) as previously described by Vainberg and colleagues (29). This observation suggests that URI and Art-27 play a role different from that canonically ascribed to prefoldin. Furthermore, URI and Art-27 do not affect AR stability and/or localization (data not shown). Importantly, URI and Art-27 strongly affect each other's stability, strengthening the idea that these two proteins interact *in vivo* in prostate cells.

URI was identified as a protein that binds RPB5, a subunit shared by all three RNA polymerases. This fact, together with the observations presented above, suggests that URI may act as a mediator to connect the transcriptional machinery to AR, possibly through Art-27. URI and Art-27 interact through the four beta-strands of their prefoldin domains (11), while Art-27 binds the androgen receptor through the two flanking alpha-helices (S. M. Markus and M. J. Garabedian, unpublished results), supporting this hypothesis. Although we were not able to coimmunoprecipitate URI with AR (Fig. 5a), Art-27 coimmunoprecipitates with AR (16). The interaction between AR and URI could be difficult to detect due to the transient nature

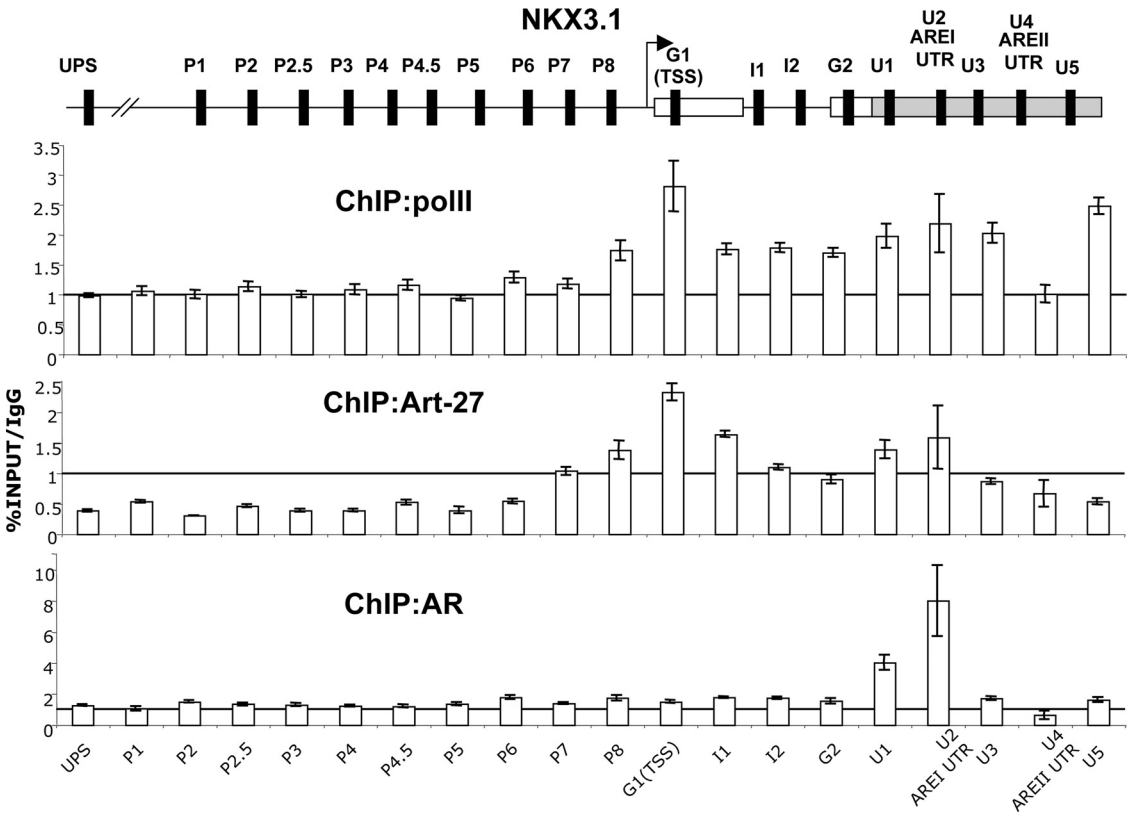

FIG. 10. Art-27 is recruited on the TSS and 3′ UTR AREI of NKX3.1. ChIP was performed as described in Materials and Methods. (Top) Scheme of the NKX3.1 gene. The regions amplified by Q-PCR after ChIP are represented by filled boxes. The open rectangles represent the 2 exons, and the shaded rectangle represents the 3′ UTR of NKX3.1. An NKX3.1 upstream region (UPS) was used as a control. (Center and bottom) Recruitment of RNA polymerase II, Art-27, and AR on the whole NKX3.1 gene and promoter. Horizontal lines at 1 indicate the control value obtained by performing ChIP using the IgG control antibody.

of the interaction, the inability of the URI antibody to recognize URI in complex with other proteins, or the instability of the complex under the conditions of the immunoprecipitation. Alternatively, there may be a pool of Art-27 protein bound to the androgen receptor but not to URI. While the precise mechanism is unclear, changes in URI mRNA expression (26) during prostate cancer progression could represent altered regulation of the AR transcriptional landscape in prostate cancer.

While URI mRNA expression is decreased in late-stage prostate cancer (26), loss of nuclear Art-27 correlated with more-aggressive disease (18). Protein expression of URI in late-stage prostate cancer has yet to be examined, but considering the interdependent expression of Art-27 and URI, it would not be surprising if the decrease in URI expression in advanced cancers correlated with loss of nuclear Art-27 and with higher tumorigenic potential. In line with this idea, we showed that URI loss affects the response of LNCaP cells to bicalutamide, a known androgen receptor antagonist (Fig. 2), and that URI overexpression decreases anchorage-independent growth of LNCaP cells (Fig. 3). Therefore, analysis of URI protein levels and regulation during prostate cancer progression could provide a functional explanation for Art-27 protein loss during the later stages of prostate cancer, offering new insights into the development of castration-resistant prostate cancers.

Previous reports (1, 3, 4) identified an R2TP/prefoldin-like complex composed of URI and Art-27, which is responsible for the cytoplasmic assembly of RNA polymerase II. In a mass spectrometry analysis of URI interactors performed by our lab using LNCaP cell lysates (J. Savas, P. Mita, J. R. Yates, and S. K. Logan, unpublished data), we also observed the interaction of URI with the R2TP/prefoldin-like complex. Interestingly, the R2TP/prefoldin-like complex shares several subunits with the R2TP complex comprising the chaperone protein p23 and the heat shock protein hsp90. The p23/hsp90 complex (R2TP complex) regulates the estrogen receptor (ER), and in particular, the small chaperone p23 was reported to affect the binding of ER to chromatin (10, 19). Moreover, a comparison of URI and p23 expression levels in the cohort of prostate tumors analyzed by Sawyers and colleagues (24) shows a very high correlation between p23 and URI (odds ratio/correlation = 23.2 [95% confidence]), suggesting a possible functional correlation between p23 and URI in prostate cells. Our focus, however, was on the role of URI as a transcription regulator. Consistent with the idea that URI is also present in the nucleus, our mass spectrometry analysis of URI nuclear interactors identified several nuclear proteins, such as RPB1 phos-

phorylated at Ser2/Ser5, MLL1, various components of the mediator complex, elongation factors, and TATA box binding protein-associated factors (TAFs), that suggest a direct role of URI and Art-27 in transcription. Moreover, the demonstrated binding of URI to the general transcription factor TFIIF and to the Paf-1 complex (30, 33) strengthens the idea that nuclear URI plays an important role in transcription regulation independent of its cytoplasmic role as a chaperone for Pol II complex assembly.

The costabilization of URI and Art-27 makes it very difficult to discern independent functions for the two proteins. Our microarray analysis of mRNA expression in LNCaP cells depleted of URI or Art-27 demonstrates substantial overlap in gene profiles due to the loss of one or the other protein. Our results indicate that URI stabilizes Art-27 protein in the cytoplasm and nuclei of prostate cells and that loss of URI decreases the level of Art-27 bound to DNA. On the NKX3.1 gene, knockdown of URI resulted in a decrease of Art-27 protein recruitment. A decrease in the repressive effects of Art-27 on AR-mediated transcription upon URI knockdown could explain the transcriptional upregulation of androgen-regulated genes such as PSA, FKBP5, and NKX3.1. Interestingly, knockdown of URI also results in increased recruitment of AR on NKX3.1 AREs. This result cannot be explained by an effect of URI on Art-27 corepressor activity and/or stability. However, the mechanisms by which Art-27 is able to repress AR transcription are still unknown. Our results (Fig. 9 and 10) suggest that URI and Art-27 could be involved in chromatin remodeling and chromatin structure, ensuring accurate recruitment of the AR to the AREs of androgen-regulated genes. This hypothesis is supported by the finding that a fraction of URI and Art-27 is bound to the chromatin in an androgen-independent manner (Fig. 9) and by previous reports indicating that URI interacts with chromatin-remodeling proteins, such as the helicases TIP49 and TIP48 (11). Our ChIP analysis of Art-27, AR, and pol II recruitment across the entire NKX3.1 gene (Fig. 10) demonstrates the recruitment of Art-27, probably in complex with URI, on the TSS and on the AREI enhancer region in the 3′ UTR of NKX3.1. These data are consistent with the reported binding of Art-27 to the AR (16) and with the binding of URI to RNA polymerase II (8, 14, 15). The data presented in this report suggest that an Art-27–URI-containing complex binds chromatin in an androgen-independent manner and that loss of this complex may affect chromatin structure, which, in turn, could be responsible for aberrant AR recruitment and transcription.

ACKNOWLEDGMENTS

Grant support was received from the NIH (R01CA112226 [S.K.L.] and W81XWH-10-1-0431 [P.M.]) and the Urologic Disease Center of Excellence at the New York University School of Medicine (S.K.L.).

REFERENCES

1. **Boulon, S., et al.** 2010. HSP90 and its R2TP/Prefoldin-like cochaperone are involved in the cytoplasmic assembly of RNA polymerase II. Mol. Cell **39:**912–924.
2. **Chen, C. D., et al.** 2004. Molecular determinants of resistance to antiandrogen therapy. Nat. Med. **10:**33–39.
3. **Cloutier, P., et al.** 2009. High-resolution mapping of the protein interaction network for the human transcription machinery and affinity purification of RNA polymerase II-associated complexes. Methods **48:**381–386.
4. **Cloutier, P., and B. Coulombe.** 2010. New insights into the biogenesis of nuclear RNA polymerases? Biochem. Cell Biol. **88:**211–221.
5. **Delgermaa, L., et al.** 2004. Subcellular localization of RPB5-mediating protein and its putative functional partner. Mol. Cell. Biol. **24:**8556–8566.
6. **Deplazes, A., N. Mockli, B. Luke, D. Auerbach, and M. Peter.** 2009. Yeast Uri1p promotes translation initiation and may provide a link to cotranslational quality control. EMBO J. **28:**1429–1441.
7. **Djouder, N., et al.** 2007. S6K1-mediated disassembly of mitochondrial URI/PP1γ complexes activates a negative feedback program that counters S6K1 survival signaling. Mol. Cell **28:**28–40.
8. **Dorjsuren, D., et al.** 1998. RMP, a novel RNA polymerase II subunit 5-interacting protein, counteracts transactivation by hepatitis B virus X protein. Mol. Cell. Biol. **18:**7546–7555.
9. **Feldman, B. J., and D. Feldman.** 2001. The development of androgen-independent prostate cancer. Nat. Rev. Cancer **1:**34–45.
10. **Freeman, B. C., S. J. Felts, D. O. Toft, and K. R. Yamamoto.** 2000. The p23 molecular chaperones act at a late step in intracellular receptor action to differentially affect ligand efficacies. Genes Dev. **14:**422–434.
11. **Gstaiger, M., et al.** 2003. Control of nutrient-sensitive transcription programs by the unconventional prefoldin URI. Science **302:**1208–1212.
12. **Guicciardi, M. E., and G. J. Gores.** 2008. Cell stress gives a red light to the mitochondrial cell death pathway. Sci. Signal. **1:**pe9.
13. **Jeronimo, C., et al.** 2007. Systematic analysis of the protein interaction network for the human transcription machinery reveals the identity of the 7SK capping enzyme. Mol. Cell **27:**262–274.
14. **Kirchner, J., et al.** 2008. *Drosophila* Uri, a PP1α binding protein, is essential for viability, maintenance of DNA integrity and normal transcriptional activity. BMC Mol. Biol. **9:**36.
15. **Le, T. T., et al.** 2005. Mutational analysis of human RNA polymerase II subunit 5 (RPB5): the residues critical for interactions with TFIIF subunit RAP30 and hepatitis B virus X protein. J. Biochem. **138:**215–224.
16. **Markus, S. M., et al.** 2002. Identification and characterization of ART-27, a novel coactivator for the androgen receptor N terminus. Mol. Biol. Cell **13:**670–682.
17. **Mellinghoff, I. K., and C. L. Sawyers.** 2004. TORward AKTually useful mouse models. Nat. Med. **10:**579–580.
18. **Nwachukwu, J. C., et al.** 2009. Genome-wide impact of androgen receptor trapped clone-27 loss on androgen-regulated transcription in prostate cancer cells. Cancer Res. **69:**3140–3147.
19. **Oxelmark, E., et al.** 2006. The cochaperone p23 differentially regulates estrogen receptor target genes and promotes tumor cell adhesion and invasion. Mol. Cell. Biol. **26:**5205–5213.
20. **Parusel, C. T., E. A. Kritikou, M. O. Hengartner, W. Krek, and M. Gotta.** 2006. URI-1 is required for DNA stability in *C. elegans*. Development **133:**621–629.
21. **Rai, J. S., M. J. Henley, and H. L. Ratan.** 2010. Mammalian target of rapamycin: a new target in prostate cancer. Urol. Oncol. **28:**134–138.
22. **Shang, Y., M. Myers, and M. Brown.** 2002. Formation of the androgen receptor transcription complex. Mol. Cell **9:**601–610.
23. **Taneja, S. S., et al.** 2004. ART-27, an androgen receptor coactivator regulated in prostate development and cancer. J. Biol. Chem. **279:**13944–13952.
24. **Taylor, B. S., et al.** 2010. Integrative genomic profiling of human prostate cancer. Cancer Cell **18:**11–22.
25. **Thomas, M. A., D. M. Preece, and J. M. Bentel.** 2010. Androgen regulation of the prostatic tumour suppressor NKX3.1 is mediated by its 3′ untranslated region. Biochem. J. **425:**575–583.
26. **Tomlins, S. A., et al.** 2007. Integrative molecular concept modeling of prostate cancer progression. Nat. Genet. **39:**41–51.
27. **Tomlins, S. A., et al.** 2005. Recurrent fusion of TMPRSS2 and ETS transcription factor genes in prostate cancer. Science **310:**644–648.
28. **Tronnersjo, S., et al.** 2007. The jmjN and jmjC domains of the yeast zinc finger protein Gis1 interact with 19 proteins involved in transcription, sumoylation and DNA repair. Mol. Genet. Genomics **277:**57–70.
29. **Vainberg, I. E., et al.** 1998. Prefoldin, a chaperone that delivers unfolded proteins to cytosolic chaperonin. Cell **93:**863–873.
30. **Wei, W., et al.** 2003. Interaction with general transcription factor IIF (TFIIF) is required for the suppression of activated transcription by RPB5-mediating protein (RMP). Cell Res. **13:**111–120.
31. **Wysocka, J., P. T. Reilly, and W. Herr.** 2001. Loss of HCF-1-chromatin association precedes temperature-induced growth arrest of tsBN67 cells. Mol. Cell. Biol. **21:**3820–3829.
32. **Xu, Y., S. Y. Chen, K. N. Ross, and S. P. Balk.** 2006. Androgens induce prostate cancer cell proliferation through mammalian target of rapamycin activation and posttranscriptional increases in cyclin D proteins. Cancer Res. **66:**7783–7792.
33. **Yart, A., et al.** 2005. The HRPT2 tumor suppressor gene product parafibromin associates with human PAF1 and RNA polymerase II. Mol. Cell. Biol. **25:**5052–5060.